Waveguiding properties of a photonic crystal fiber with a solid core surrounded by four large air holes

M. Delgado-Pinar[1], A. Díez[1], S. Torres-Peiró[1], M. V. Andrés[1], T. Pinheiro-Ortega[2], and E. Silvestre[2]

[1]*Departamento de Física Aplicada-ICMUV, Universidad de Valencia, 46100, Burjasot, Spain*
[2]*Departamento Óptica, Universidad de Valencia, 46100, Burjasot, Spain*

Abstract: The polarization-dependent guiding properties of a hexagonal-lattice photonic crystal fiber with a solid-core surrounded by four large air holes are investigated. The appearance of a polarization dependent cutoff frequency, together with several parameters as the birefringence, the modal effective area, the group velocity dispersion and the polarization dependent loss are analyzed. A collection of fibers with different structural parameters were fabricated and characterized. An effective anti-guide structure from at least 450 nm to 1750 nm, a polarizing fiber with a polarization dependent loss of 16 dB/m at 1550 nm, and an endlessly singlemode polarization-maintaining fiber with group birefringence of 2.1×10^{-3} at 1550 nm are reported. Experimental results are compared with accurate numerical modeling of the fibers.

OCIS codes: (060.2310) Fiber optics; (060.2880) Fiber design and fabrication; (060.4005) Microstructured fibers

References and Links

1. P. St. J. Russell, "Photonic crystal fibers," Science **299**, 358 (2003).
2. A. Ortigosa-Blanch, J. C. Knight, W. J. Wadsworth, J. Arriaga, B. J. Mangan, T. A. Birks, and P. S. J. Russell, "Highly birefringent photonic crystal fibers," Opt. Lett. **25**, 1325-1327 (2000).
3. K. Suzuki, H. Kubota, S. Kawanishi, M. Tanaka, and M. Fujita, "Optical properties of a low-loss polarization-maintaining photonic crystal fiber," Opt. Express **9**, 676-680 (2001), http://www.opticsinfobase.org/oe/abstract.cfm?URI=oe-9-13-676.
4. T. P. Hansen, J. Broeng, S. E. B. Libori, E. Knudsen, A. Bjarklev, J. R. Jensen, and H. Simonsen, "Highly birefringent index-guiding photonic crystal fibers," IEEE Photon. Technol. Lett. **13**, 588-590 (2001).
5. J. R. Folkenberg, M. D. Nielsen, N. A. Mortensen, C. Jakobsen and H. R. Simonsen, "Polarization maintaining large mode area photonic crystal fiber," Opt. Express **12**, 956-960 (2004).
6. A. Ortigosa-Blanch, A. Diez, M. Delgado-Pinar, J. L. Cruz, and M. V. Andres, "Ultrahigh birefringent nonlinear microstructured fiber," IEEE Photon. Technol. Lett. **16**, 1667-1669 (2004).
7. W. Belardi, G. Bouwmans, L. Provino, and M. Douay, "Form-induced birefringence in elliptical hollow photonic crystal fiber with large mode area," IEEE J. Quantum Electron. **41**, 1558-1564 (2005).
8. J. R. Folkenberg, M. D. Nielsen and C. Jakobsen, "Broadband single-polarization photonic crystal fiber," Opt. Lett. **30**, 1446-1448 (2005).
9. T. Schreiber, H. Schultz, O. Schmidt, F. Röser, J. Limpert, and A. Tünnermann, "Stress-induced birefringence in large-mode-area micro-structured optical fibers," Opt. Express **13**, 3637-3646 (2005), http://www.opticsinfobase.org/oe/abstract.cfm?URI=oe-13-10-3637.
10. H. Kubota, S. Kawanishi, S. Koyanagi, M. Tanaka, and S. Yamaguchi, "Absolutely single polarization photonic crystal fiber", IEEE Photon. Technol. Lett. **16**, 182-184, (2004).
11. J. Ju, W. Jin and M. S. Demokan, "Design of single-polarization single-mode photonic crystal fiber at 1.30 and 1.55 μm," J. Lightwave Technol. **24**, 825-830 (2006).
12. K. Saitoh and M. Koshiba, "Single-polarization single-mode photonic crystal fibers," IEEE Photon. Technol. Lett. **15**, 1384-1386 (2003).
13. M. Delgado-Pinar, A. Diez, J. L. Cruz, and M. V. Andres, "High extinction-ratio polarizing endlessly single-mode photonic crystal fiber," IEEE Photon. Technol. Lett. **19**, 562-564 (2007).
14. S. G. Johnson and J. D. Joannopoulos, "Block-iterative frequency-domain methods for Maxwell's equations in a planewave basis," Opt. Express **8**, 173-190 (2001), http://www.opticsexpress.org/abstract.cfm?URI=OPEX-8-3-173, MIT Photonic-Bands package available at: http://ab-initio.mit.edu/wiki/index.php/MIT_Photonic_Bands

#105849 - $15.00 USD Received 5 Jan 2009; revised 6 Feb 2009; accepted 7 Feb 2009; published 13 Apr 2009

15. N. A. Mortensen, "Effective area of photonic crystal fibers," Opt. Express **10**, 341-348 (2002), http://www.opticsinfobase.org/oe/abstract.cfm?URI=oe-10-7-341.
16. B. T. Kuhlmey, R. C. McPhedran, and C. M. de Sterke, "Modal cutoff in microstructured optical fibers," Opt. Lett. **27**, 1684-1686 (2002).
17. E. Silvestre, T. Pinheiro-Ortega, P. Andres, J. J. Miret, and A. Ortigosa-Blanch, "Analytical evaluation of chromatic dispersion in photonic crystal fibers," Opt. Lett. **30**, 453-455 (2005).
18. R. B. Dyott, *Elliptical Fiber Waveguides* (London: Artech House, 1995).

1. Introduction

In the last years, microstructured optical fibers (MFs) have attracted much interest among researchers. These fibers have shown remarkably new properties and can outperform conventional fibers in some respects [1]. The guiding properties can be engineered by adjusting the geometrical parameters of the microstructure. In particular, different approaches to realize polarization-maintaining (PM) MFs have been experimentally reported [2-7]. PM-MFs with modal birefringence of an order of magnitude higher than conventional fibers have been experimentally demonstrated. One of the most successful PM-MFs was first reported by Suzuki et al. [3]. It was a solid-core hexagonal-lattice MF, in which two opposite holes of the first ring were enlarged. In this fiber, the birefringence arises from the effective index difference between the two linear polarization modes. Several approaches of PM-MFs based on stress-induced birefringence have also been reported [5].

Recently, it has been demonstrated that PM-MFs can be designed to exhibit single-mode and single-polarization (SP) guidance, so that they allow the propagation of one polarization mode while the orthogonal polarization mode is radiated. Applications of SP fibers include its use in fiber sensor systems, telecommunications and fiber lasers. Several experimental demonstrations of SP-MFs based on stress-induced birefringence have been reported. In one design, two stress-applying parts were placed opposite to each other in the silica jacket [8] while in a second approach, index-matched stress applying elements were included in the photonic cladding [9]. Both fibers exhibit a certain bandwidth at the short-wavelength edge of the transmission window where only one polarization propagates.

SP-MFs based on form-induced birefringence have also been reported. In particular, the MF approach reported in [3] can be designed for SP operation, as it was demonstrated experimentally by Kubota et al. [10]. A detailed theoretical analysis and some design rules for such an SP-MF can be found in [11]. Saitoh et al. [12] proposed and theoretical analyzed an SP-MF based on the same operation principle, but including four large air holes in the inner ring instead of only two. Such a design involves similar fabrication efforts, but it has the advantage that reduces the confinement loss of the slow mode in the SP wavelength band. In a previous paper, we presented the fabrication and experimental characterization of a polarizing MF based on such a structure. An extinction ratio of 16 dB/m at 1550 nm was reported [13].

Here, the analysis of the guiding properties of such PM-MF is extended and some design details are given. For a given wavelength, this type of PM-MF presents different polarization guiding regimes as a function of the structural parameters. In particular, it can be designed to be (1) a high birefringence PM-MF that guides the two polarization eigenstates of the fundamental mode, (2) a SP-MF, in which only one polarization mode is guided, or (3) an effective anti-guide MF that does not support any mode at all. In this paper, we complement the experimental results on polarization dependent attenuation presented in [13] and we report an anti-guide fiber from at least 450 nm and a high birefringence endlessly singlemode PM-MF. All of them are based on the structure described above, i.e., the fiber with a photonic crystal cladding and a solid core surrounded by four large air holes. Some experimental results regarding a polarizing MF [13] are also included for completeness. Finally, experimental results are compared with accurate numerical modeling of the fibers.

2. Operation principle

The inset of Fig.1 shows a diagram of the ideal geometry of the fiber that we discuss in this section. Regarding the periodic structure of small air holes with diameter d and pitch Λ, the four large air holes of diameter D together with the solid core can be described as a defect that

#105849 - $15.00 USD Received 5 Jan 2009; revised 6 Feb 2009; accepted 7 Feb 2009; published 13 Apr 2009

breaks the regularity and gives rise, eventually, to the appearance of localized states, i.e., guided modes. This defect has a relatively complex structure that leads to some peculiar polarization and wavelength dependent properties.

The introduction of the large air holes near the solid core is expected to cause two effects on the guiding properties of the fiber. First, the microstructure becomes anisotropic and also the solid core becomes elliptic. As a result, the two polarization eigenstates of the fundamental mode will propagate with different phase velocity, hence, the fiber becomes birefringent. Second, compared to a solid-core regular MF, the average refractive index of the defect is decreased and this causes that the modal index of the fundamental mode also decreases. More specifically, the modal indices of the two polarization eigenstates of the fundamental mode are lower than the modal index of the fundamental mode of the corresponding regular MF with solid core and no large air holes. Thus, for a constant value of D/Λ, when the air filling fraction of the periodic structure decreases –i.e., the ratio d/Λ decreases–, the cladding effective index –i.e., the envelope of the radiation modes– moves upwards to higher values. It may happen that the dispersion curves of the polarization modes intersect the cladding effective index forcing the cutoff of the modes. This behaviour can be understood if we analyze the properties of the complex defect of the fiber as a function of wavelength. For short wavelengths, the fields are tightly confined in the silica region of the defect and so the modal index is higher than the effective index of the cladding. For long wavelengths, however, the fields overlap the large holes and hence the modal index is lower. Since $D > d$, the modal index of the modes can be lower than the cladding effective index. Finally, because of the birefringence, the cutoff wavelength is different for each polarization mode, so there is a wavelength band where the fiber guides only one polarization.

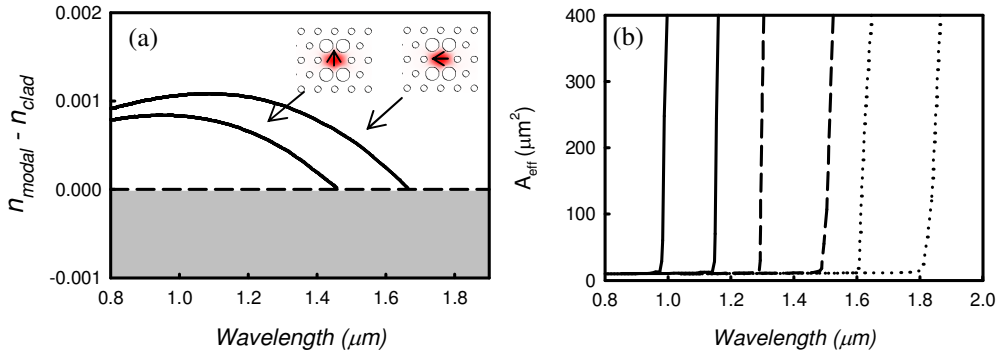

Fig. 1. (a) Difference between the modal index and the cladding effective index, for the two polarization eigenstates of the fundamental mode. $D/\Lambda = 0.8$, $d/\Lambda = 0.39$, $\Lambda = 3.3$ μm. Inset shows the microstructure of the fiber and the mode intensity pattern. The orientation of the electric field is indicated. (b) Effective area of the two polarization modes vs. wavelength. $D/\Lambda = 0.8$, $\Lambda = 3.3$ μm. $d/\Lambda = 0.36$ (solid line), $d/\Lambda = 0.38$ (dashed line), and $d/\Lambda = 0.4$ (dotted line).

The calculations shown in this section (figures 1 and 2) were carried out using the MIT Photonic-Bands package [14]. This package computes frequency eigenstates of Maxwell's equations in periodic dielectric structures using preconditioned block-iterative eigensolvers in a planewave basis [14]. The method assumes periodic boundary conditions. A supercell of 7x7 periods was used for the simulations.

Figure 1(a) shows the modal index of the two polarization eigenstates of the fundamental mode for a given fiber. For clarity, the difference between the modal indices and the cladding effective index is shown. The orientation of the electric field of each eigenstate is indicated. The electric field of the fast mode is orientated along the short axis of the elliptic core, while it is oriented along the long axes for the slow mode. It can be distinguished three guidance regimes. At short wavelengths, the two eigenstates propagate in accordance with their own phase velocity. The fiber birefringence increases with optical wavelength; in this example

#105849 - $15.00 USD Received 5 Jan 2009; revised 6 Feb 2009; accepted 7 Feb 2009; published 13 Apr 2009

from 2.4×10^{-4} at 1 μm up to 6×10^{-4} at 1.4 μm. For this particular example the birefringence regime extends up to 1.45 μm. At this wavelength, the modal index of the fast mode reaches the cladding effective index and it is cutoff. Within a wavelength band, that in this case extends up to 1.65 μm, the fast mode is cutoff while the slow mode still propagates. Hence, the fiber exhibits single-mode single-polarization (SP) guiding regime. Beyond 1.65 μm the slow mode is also cutoff and the fiber does not support any guided mode at all, although an MF with the same d/Λ and no large air holes would guide the fundamental mode. These results demonstrate that simple qualitative models to explain guidance in MF with solid cores in terms of total internal reflection have important limitations. In the case of the MF that we consider here, one could conclude that the presence of the large air holes should reinforce the total internal reflection of light confined in the solid core, while in fact the guidance is cutoff.

Figure 1(b) shows theoretical calculations of the effective area of the two polarization eigenstates of the fundamental mode for different fibers. The cutoff of the modes is clearly acknowledged by a sharp increase of the effective area. For a fixed value of D/Λ, the SP wavelength band shifts to longer wavelengths and it becomes wider as the air-filling fraction of the microstructured cladding is increased. A similar trend was found when d/Λ was fixed and the diameter of the large holes was decreased.

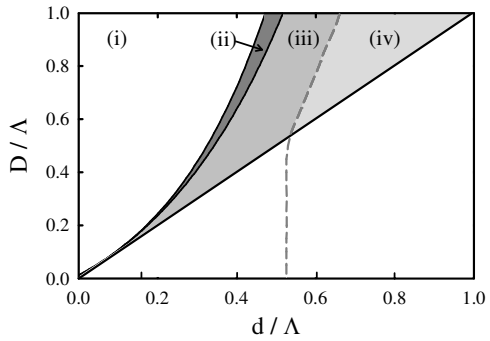

Fig. 2. Map of guided modes as a function of the structural parameters at a fix normalized frequency $\Lambda/\lambda = 2$. The dashed line indicates the cutoff of the first high-order mode. The diagonal line corresponds to a regular MF.

Figure 2 is a map of the guidance regimes as a function of the geometric parameters, at a fix normalized frequency $\Lambda/\lambda = 2$. The mode effective area has been used to determine the cutoff of the different modes, as it is detailed in [15]. The diagonal line represents fibers with $D = d$, i.e., microstructured fibers with regular hexagonal lattice of air holes in which the two polarization eigenstates are degenerated because of the symmetry of the microstructure. The area below the diagonal line correspond to fibers with the four holes smaller than the rest of holes ($D < d$). These are birefringent fibers [2] but with no polarizing or cutoff properties and they are not the scope of this paper.

The dashed line indicates the cutoff of the first higher-order mode at this normalized frequency. Thus, fibers whose structural parameters are at the right side of this line (region iv) are multimode. It is worth to note that below the diagonal line, the first high-order mode cutoff happens at a nearly constant value $d/\Lambda = 0.53$, no matter the value of D/Λ. However, above the diagonal line, the increase of D/Λ causes the cutoff to occur at larger values of d/Λ, and so the single-mode feature of the fiber is preserved for larger air-filling fractions of the microstructured cladding. The increase of the large air-holes, while the rest of parameters are kept constant, causes the decrease of the modal index of all the guided modes. Hence, the first higher-order mode is cutoff at a shorter wavelength, i.e., a longer normalized frequency. Thus, a higher value of d/Λ is required for the mode to be cutoff at $\Lambda/\lambda = 2$. Another consequence is that the well-known upper limit of d/Λ for endlessly singlemode operation in regular

#105849 - $15.00 USD Received 5 Jan 2009; revised 6 Feb 2009; accepted 7 Feb 2009; published 13 Apr 2009

triangular microstructured fibers, i.e., $d/\Lambda = 0.43$ [16], is not applicable for the fiber reported here. In fact, it is no longer a constant value but it does depend on D/Λ and endlessly singlemode regime can be found in MFs with d/Λ above that value.

Above the diagonal line, several regions of interest are indicated. The region labeled as (iii) corresponds to fibers that guide the two polarization eigenstates of the fundamental mode. With the exception of the points on the diagonal, in these fibers the propagation factor of the two polarization modes is different, so they are birefringent fibers. For a fixed value of d/Λ, the birefringence increases as the diameter of the big holes becomes larger. At the opposite side, the region (i) describes fibers that do not guide any mode at all at the wavelength of calculation. It is worth to note that microstructured fibers with d/Λ values located in this region (i), but with all the holes of the same size ($D = d$) would be guiding fibers. Finally, between both regions, there is a particularly interesting region (ii) which fulfils the conditions for the propagation of, strictly, only one polarization mode. The fast polarization mode is cutoff and only the slow mode is guided. Hence, fibers whose geometric parameters belong to this region are purely single-mode and single-polarization at the normalized frequency of the calculations.

In the experimental realization of this kind of fibers, where the number of rings is finite, confinement loss plays an important role. Near its cutoff wavelength, a mode shows high losses due to weak fields' confinement. As a result, significant polarizing effects can be observed in these fibers for wavelengths shorter that the cutoff wavelength of the fast-axis polarization mode, although, this mode is not strictly cutoff.

3. Fabrication of the fibers

The fibers were fabricated by the stack-and-draw technique. Silica capillaries of 1.5 mm outer diameter and 0.375 mm wall thickness were stacked together to form a hexagonal lattice with 5 rings of air-holes. The central capillary was replaced by a solid silica rod, and four capillaries of the first ring were replaced by capillaries with the same outer diameter but a thinner wall-thickness of 0.115 mm. The stack was jacketed and pulled down to obtain the preforms. In a second step, the preforms were pulled down to optical fiber of about 100 μm diameter. During the fiber drawing, different fibers were fabricated by changing slightly the drawing conditions, i.e., the furnace temperature and the gas overpressure within the holes. Figure 3(a) shows an SEM image of one of the fibers fabricated. The inflation of the holes during the fabrication process distorted slightly the structure in the vicinity of the core, so that the distance between two adjacent large holes, as well as D, are a bit larger than the pitch Λ (measured in the outer rings).

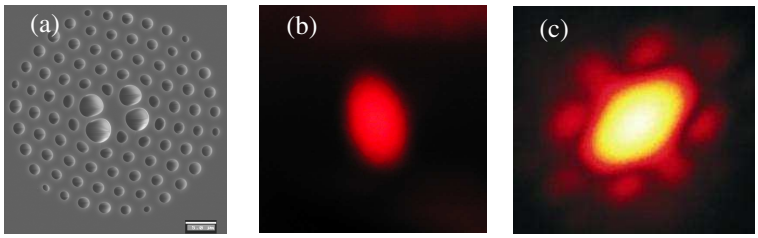

Fig. 3. (a) SEM image of fiber 3. (b)-(c) Output far-field pattern at 633 nm of fiber 1 and fiber 3, respectively, under similar illumination conditions. Fiber length 10 cm and 2 m, respectively.

4. Experimental results and discussion

In this section, we present the experimental characterization of three fibers that were chosen to illustrate the different guiding regimes described in the previous section. Table 1 summarizes their structural parameters. In this series of fibers, the ratio D/Λ is practically constant while the ratio d/Λ varies from 0.30 to 0.48.

#105849 - $15.00 USD Received 5 Jan 2009; revised 6 Feb 2009; accepted 7 Feb 2009; published 13 Apr 2009

In order to model accurately the properties of the fabricated fibers, taking into account the real geometry of the microstructure, we followed the method described in [17]. This technique allows fast and accurate analysis of realistic microstructured fibers by combining an iterative Fourier method and the implementation of an edge-detection algorithm. This approach permits dealing with arbitrary spatial refractive-index distributions. The spatial refractive-index distribution used for the simulations of the fabricated fibers (results are shown in figures 4 and 5) were obtained from SEM images of the fibers' cross sections. The five rings of holes with their real shape were taken into account. Outside the holes region the MF was enclosed in a jacket of silica surrounded by air.

Table 1. Structural parameters of the fiber: pitch of the regular lattice (Λ), diameter of the holes of the regular lattice (d), diameter of the large holes (D), and core diameter (long/short side).

	Λ (μm)	D/Λ	d/Λ	Core Size (μm) long/short axes
Fiber 1	3.53	1.06	0.30	5.13 / 2.54
Fiber 2	3.62	1.06	0.36	6.67 / 4.06
Fiber 3	3.13	1.01	0.48	5.94 / 3.84

The guidance properties of the three fibers were experimentally investigated. A first inspection was done by launching red light into the fibers and looking at the fibers' output intensity pattern. In the case of fiber 1 no light was propagated in the core after a section of few cm regardless of the input polarization orientation. Most of the light power launched into the core spread out into the cladding after few milimeters. Figure 3 (b) shows the far-field intensity pattern for a 10 cm long section of fiber. Index matching oil was used to strip out the light propagating in the cladding. This image must be compared with Fig. 3 (c), which shows the far-field intensity pattern from fiber 3 under similar illumination conditions and a longer section of fiber of 2 meters (notice that the camera was saturated, in this case). Hence, it can be concluded that fiber 1 did not guide at 633 nm. Theoretical calculations carried out for this fiber predicted no guidance from at least 400 nm.

The near-field intensity pattern of fibers 2 and 3 had elliptical shape with the same orientation than the fiber core. At 633 nm, no evidence of higher order modes was observed for these two fibers, even when short pieces of less than 10 cm long were used. To check the singlemode propagation at shorter wavelengths, we attempted the cutoff wavelength measurement for higher order modes by the bend-reference technique using a halogen lamp and an OSA. However, no mode cutoff was observed from at least 450 nm.

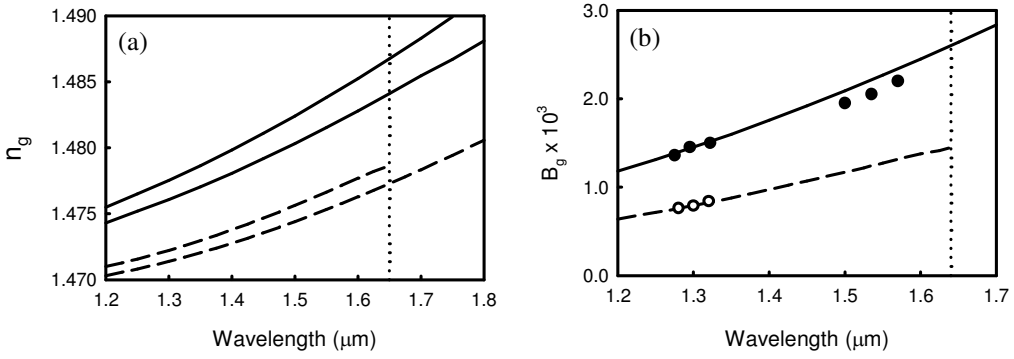

Fig. 4. (a) Calculated group index of the two polarization guided modes of fiber 2 (dashed line) and fiber 3 (solid line). The vertical dotted line indicates the theoretical cutoff of the fast mode of fiber 2. (b) Group birefringence vs. wavelength. Lines are the theoretical results for fiber 2 (dashed line), and fiber 3 (solid line). Dots are experimental data.

#105849 - $15.00 USD Received 5 Jan 2009; revised 6 Feb 2009; accepted 7 Feb 2009; published 13 Apr 2009

The polarization guiding properties of fibers 2 and 3 were investigated. Light provided by a broadband unpolarized light source was launched into the fibers through a linear polarizer, which allowed rotating the polarization orientation of the input signal. In the case of fiber 2, light transmission changes were observed at wavelengths longer than 1.2 μm as the input polarization was rotated. Between 1.2 μm and 1.45 μm the polarization dependent loss (PDL) per unit length was moderate, for example at 1.3 μm the PDL was 2.5 dB/m. However, the PDL increased sharply for wavelengths above 1.45 μm. In particular, at 1550 nm a PDL of 16 dB/m was measured, while the transmission loss of the slow mode was 0.9 dB/m. More details of the experimental characterization of this fiber can be found in [13]. Theoretical modeling of this fiber yields the cutoff wavelength of the fast mode around 1.65 μm (see Fig. 4(a)). This is not in disagreement with the experimental results since confinement loss must be also taken into consideration. Actually, the polarizing properties at wavelengths shorter than cutoff are due to the large confinement loss that affects the fast polarization mode even at wavelengths well below cutoff. This behaviour was predicted theoretically for single-polarization MFs based on similar structures [11].

In the case of the fiber 3, the light transmission was practically independent on the input polarization orientation, at least within our experimental measurement wavelength range from 450 to 1750 nm. The transmission losses of both polarization modes were moderate, about 0.65 dB/m at 1550 nm, and the PDL value was negligible. This agrees with the theoretical modeling results, which indicate that the two polarization modes are guided up to at least 2 μm (see Fig. 4). Therefore, fiber 3 is single-mode and polarization-maintaining from 450 to 1750 nm.

The group birefringence B_g of fibers 2 and 3 was measured around 1.3 μm using the modal interferometer method [18]. Since this measurement technique requires short pieces of fiber (few tens of cm), the birefringence of fiber 2 could also be measured at this wavelength. B_g of fiber 3 was also measured around 1550 nm using the frequency-domain modulated-carrier method [18] (tpycally, several meters of fiber are required). Figure 4(b) shows the experimental measurements of B_g for both fibers, along with the results obtained from the theoretical modeling. The agreement between theory and experimental results is quite good. We would like to remark the large B_g of fiber 3. For example, at 1550 nm, $B_g = 2.1\times10^{-3}$, which is, to our knowledge, one of the largest B_g reported for an endlessly singlemode MF.

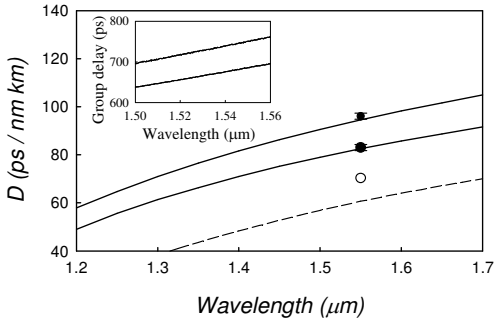

Fig. 5. Group velocity dispersion (D) vs. wavelength. Lines are the theoretical results for the slow mode of fiber 2 (dashed line), and for both polarization modes of fiber 3 (solid line). Dots are experimental data. Inset shows the measurement of group delay vs. wavelength for the two polarization modes of fiber 3 (fiber length 9.5 m).

The frequency-domain modulated-carrier method provides the group delay vs. wavelength of a light beam propagating along a given fiber length. Therefore, the group velocity dispersion D of the guided modes can also be obtained from this technique since:

#105849 - $15.00 USD Received 5 Jan 2009; revised 6 Feb 2009; accepted 7 Feb 2009; published 13 Apr 2009

$$D = \frac{1}{L}\frac{d\tau}{d\lambda} \tag{1}$$

where τ is the group delay, λ is the wavelength and L is the length of fiber used for the measurement. Inset of Fig. 5 shows the group delay as a function of wavelength for the two polarization modes of fiber 3. At 1.55 μm, the dispersion of the slow and fast mode was 82.9 ps/nm·km and 95.9 ps/nm·km, respectively. Experimental and theoretical results are compared in Fig. 5. The theoretical calculations indicate that the zero dispersion wavelength of the two polarization modes (not plotted in Fig. 5) are around 890 and 910 nm, respectively. The dispersion of the slow mode of fiber 2 was also measured and the result is included in Fig. 5.

5. Conclusions

The waveguiding properties of a hexagonal-lattice photonic crystal fiber with a solid-core surrounded by four large air holes were investigated. We provide a design map to obtain different polarization guiding regimes as a function of the structural parameters. Within a given wavelength range, the fiber can be designed either to be an anti-guide, or a single-mode single-polarization fiber, or a highly birefringent fiber. Some important limitations of simple models broadly used for solid core photonic crystal fibers, based on total internal reflection guidance, have been pointed up and discussed. Our experimental work illustrates these guiding regimes. Here, we have reported a collection of fibers, including a fiber that is an anti-guide from at least 450 nm to 1750 nm, a polarizing fiber with a polarization dependent loss of 16 dB/m at 1550 nm and an endlessly singlemode polarization-maintaining fiber with group birefringence of 2.1×10^{-3} at 1550 nm. Experimental results were compared with accurate numerical modeling that takes into account the real structural parameters of the fibers, showing good agreement.

Acknowledgments

This work has been financially supported by the Ministerio de Educación y Ciencia of Spain (projects TEC2008-05490).

#105849 - $15.00 USD Received 5 Jan 2009; revised 6 Feb 2009; accepted 7 Feb 2009; published 13 Apr 2009